Wake Transitions of Rolling and Sliding Cylinders and Spheres

Anirudh Rao[1,3], Bronwyn E. Stewart[1,2], Mark C. Thompson[1,3], Thomas Leweke[2] &
Kerry Hourigan[1,3]

[1]*Fluids Laboratory for Aeronautical and Industrial Research, Monash University, Melbourne 3800, Australia*
[2]*Institut de Recherche sur les Phénomènes Hors Equilibre, CNRS/Universités Aix-Marseille, Marseille, France*
[3]*Division of Biological Engineering, Monash University, Melbourne 3800, Australia*

ABSTRACT

Flow is predicted around the generic 2d and 3d bluff bodies, the cylinder and the sphere, for different forward or reverse rotation rates on a plane wall, using a high-order spectral element method. Dye visualisation is undertaken to validate the predictions. The Reynolds number ranges are [20, 500] and [100, 350] for the cylinder and sphere, respectively. The combined effects of the nearby wall and the imposed body motion have been analysed with respect to the dominant transitions in the wakes. For the cylinder, the forward rolling motion is shown to destabilise the wake flow, while reverse rotation delays the onset of unsteady flow. For the sphere, four primary wake modes, plus an additional unsteady mode, are identified. Good qualitative agreement is observed between the numerical and experimental results. Predictions of the wakes of cylinders in tandem rolling on a wall are presented, noting the interference effects as the rotation rate and separation distance are varied.

INTRODUCTION

The flow around a single, stationary, non-spinning bluff body in a free stream has been well investigated. Initial studies by Roshko (1954) investigated the vortex shedding behind a cylinder, and the variation of the shedding frequency as function of Reynolds number was recorded. Two regimes of flow were identified: one below Re = 150 and the other at Re = 300, where an irregular shedding was detected. Williamson (1989) identified the modes of shedding that appear as the Reynolds number is increased to 300: Mode A shedding occurs at Re = 180 and has a spanwise wavelength of 4 cylinder diameters; Mode B shedding has a smaller spanwise wavelength of approximately 1 diameter, with an intermediate transition regime where the two modes co-exist. Three-dimensional flow was computed numerically by Thompson *et al.* (1996), and the vortex structures present throughout the transition regime were presented.

For the flow around a sphere, the flow remains attached to the surface until Re ≈ 20 is reached (Pruppacher *et al.,* 1970). As the Reynolds number increases, the flow behind the sphere undergoes a transition from steady axisymmetric to steady asymmetric flow. Studies have found that this transition occurs at Re ≈ 210 (Magarvey & Bishop, 1961). Various numerical and experimental works have observed the transition to unsteady flow to occur at 270 < Re < 280 (Ormières & Provansal, 1999).

There have been various studies of bluff bodies spinning in isolation (e g., Mittal, 2004), spinning near but not on a wall (e.g., Cheng & Luo, 2007), or non-spinning near a wall (e.g., Bearman & Zdravkovich, 1978), or a rolling cylinder study by Bhattacharyya *et* al. (2004) restricted to a steady flow. However, there has been limited investigation of the unsteady and three-dimensional wake transitions of bluff bodies combining both translation and spinning on, or very close to, a wall.

In the current study, the flow around cylinders and spheres rolling, in a prograde, retrograde or sliding sense, is predicted and observed. In addition to being of importance for fundamental fluid mechanics and aeronautics (as well as *le foot* and *pétanque*!), the problem of spherical bodies moving relative to fluid at low Reynolds numbers is of interest to biomedical applications, such as leukocyte migration or cell culture in bioreactors. The transition of the wakes from steady to unsteady and from two- to three-dimensional is investigated via direct numerical simulations, experiments and linear stability study (cylinder). A body moving near a wall will experience both a wall-induced lift force and a Magnus lift if it is spinning. Additionally, the presence of a second body in tandem can lead to interference effects on the wakes. The main aim is to evaluate the effect of the presence of the wall on the Reynolds numbers at which the transitions occur and the structure of the wakes following transition for a range of rotation rates.

METHODOLOGY

The present investigation concerns the flow around one or two cylinders or spheres moving along a wall, with a range of imposed rotation rates. Particular attention is given to the steady and unsteady structures that develop in the wake and the transition to three-dimensions. How these flows are altered by the combined effects of translation and rotation when the body is in near-contact with a wall can then be determined.

The problem setup is shown in Fig. 1. When a rotational motion is imposed on the cylinder(s) or sphere(s), the non-dimensional rotation rate may be defined as $\alpha = D\omega / 2U$, where ω and U are the angular and translational velocities,
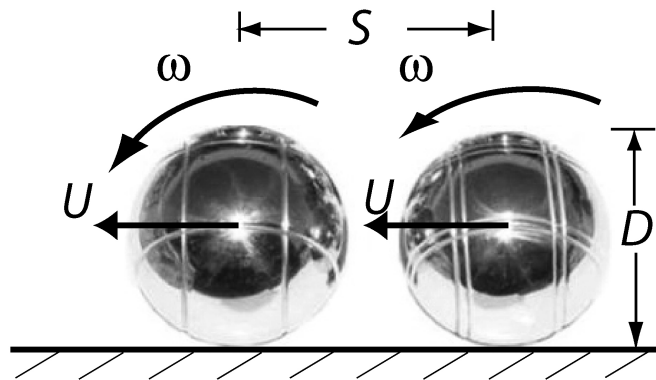
Figure 1: Schematic of cylinders or spheres rolling on a plane wall.

respectively, of the one or more bodies, D is the diameter of the body, and S is the spacing between body centres.

The numerical scheme solves the viscous, incompressible Navier-Stokes equations, assuming an incompressible, Newtonian fluid. The equations are discretised with the use of a semi-implicit spectral element scheme that incorporates time-splitting for the temporal discretisation, which takes place via a fractional step method (see Karniadakis *et al.*, 1991). More details, with boundary conditions, are provided in Stewart *et al.* (2008, 2010a,b).

Together with the numerical simulations, an experimental study was also undertaken in a water tunnel equipped with a moving floor and boundary layer suction. Fluorescein dye was injected into the flow upstream of the sphere, either on the moving floor or through a narrow tube positioned in the free stream far from the body. The dye was then illuminated with the light from an argon laser, allowing visualization of the wake either as a volume or in a plane.

RESULTS AND DISCUSSION
Cylinders, spheres rolling on wall

Single body
In Fig. 2, the predicted and visualized wakes of the cylinder are shown for Re = 80/90 and 400/450, where the Reynolds number Re is based on U and D. Retrograde rolling is seen to flatten the wake substantially. The sense and rate of rolling will be seen later to affect the Reynolds number at which transition to unsteadiness occurs.
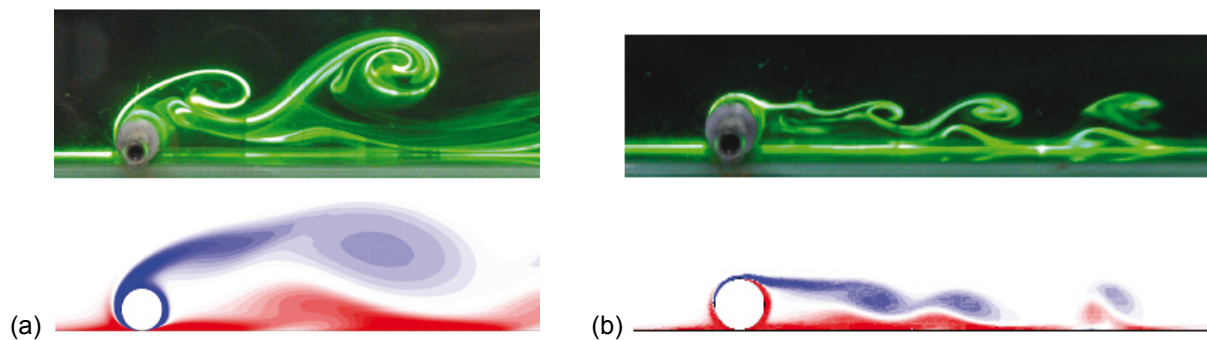

Figure 2: A comparison of dye visualizations with numerical predictions of vorticity fields for the unsteady regime of the cylinder wake. (a) Top: Experimental visualization (Re = 80); bottom: numerical vorticity prediction (Re = 90). α = 1 (prograde rolling). (b) Top: Experimental visualization (Re = 450); bottom: numerical vorticity prediction (Re = 400). α = -1 (retrograde rolling).

As Re increases, the wake experiences a transition to unsteady flow. Again, the structures in the wake are dependent on the rotation rate, and two distinct unsteady modes are observed. For the cases of α > 0 (prograde rolling), the recirculation zone behind the sphere undergoes a transition with increasing Re and vortex shedding begins. This takes the form of hairpin vortices, as for the isolated sphere, and an example of the wake is shown in figure 3(a). As distinct from the sphere in an unbounded flow, the proximity of the moving wall fixes the orientation of the wake, with the hairpin vortices forming over the top of the sphere and tilting away from the wall as they move downstream. The sense of rotation of the hairpin vortices is the same as for the vortex shedding from an isolated sphere.

When the Reynolds number of the flow is increased during the numerical simulations for retrograde rolling, α = −1, an interesting observation is made. The flow undergoes a bifurcation to an unstable solution branch which is not detected in the experiments. When allowed to develop in the absence of any noise, the reversed rolling wake develops into an unsteady symmetric mode. However, an additional symmetric mode was found that is unstable to white noise, changing to a stable antisymmetric mode (Fig. 4).
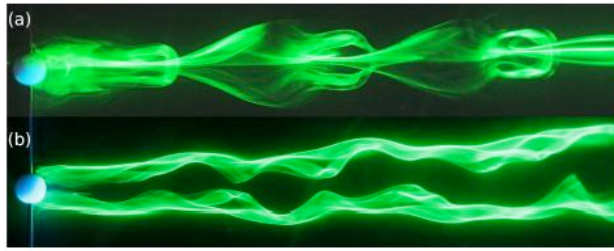
Figure 3: Dye visualization of unsteady wake flows at Re = 200 behind (a) the forward rolling sphere with $\alpha = 1$, showing the shedding of hairpin vortices, and (b) the reversed rolling sphere with $\alpha = -1$, in which a transverse motion of the streamwise vortices is present.
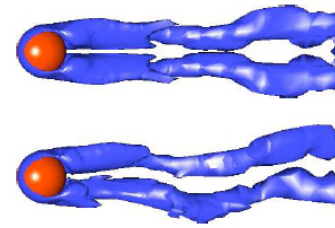

Figure 4: Predicted wake modes of a sphere for $\alpha = -1$, Re = 300, showing an unstable mode. Top: Unstable symmetric wake mode of sphere. Bottom: Stable antisymmetric wake mode following a perturbation (white noise) to the flow.

The transition to unsteadiness for the flow around the cylinder has been determined (Fig. 5). Contrary to the cylinder wake behaviour, the Reynolds number of the wake of a sphere at transition to unsteadiness varies non-monotonically with change of rotation rate, and is generally lower than for the non-rotating ($\alpha = 0$, sliding) case (Fig. 6).
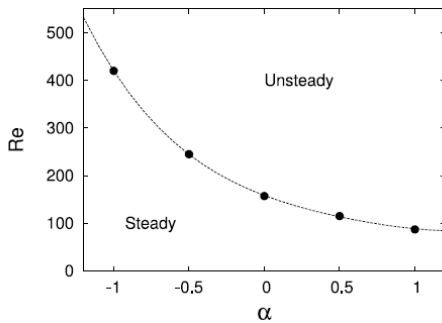

Figure 5: Transition from steady to unsteady flow around a cylinder for varying rotation rate, as predicted from the two-dimensional simulations.
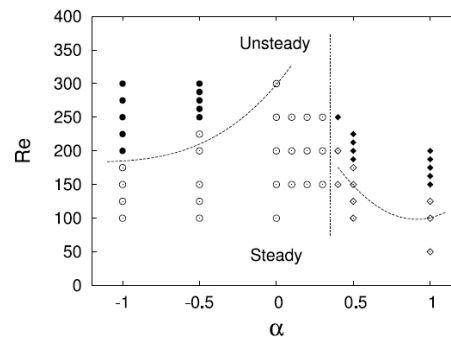

Figure 6: Transition map of the predicted four different wake modes of the sphere for varying rotation rates. Closed symbols indicate unsteady modes and open symbols denote steady modes. The steady wake mode for $\alpha > 0$, and the corresponding unsteady mode displaying the shedding of hairpin vortices, are given by $\blacklozenge$ and $\lozenge$, respectively. Alternatively, the steady mode for $\alpha \leq 0$, comprising counter-rotating streamwise vortices and the associated antisymmetric mode are given by $\circ$ and $\bullet$, respectively. The dashed curves indicate the experimentally determined boundaries.

For the rolling cylinder, a Floquet linear stability analysis has been used to predict the transition of the flow to three-dimensionality. The boundaries (contours of neutral stability) between two- and three-dimensional flow with varying Re are plotted for each α in Figure 7. For Reynolds numbers to the left of these contours, the flow is steady and two-dimensional, while to the right, the flow is steady and three-dimensional. The present study finds that, for each of the 5 values of rotation rate α, a three-dimensional mode will grow at a Reynolds number below the predicted onset of unsteadiness, and provides the wavelength, λ, at which the growth rate is maximum. Direct numerical simulations of the three-dimensional flows have also been undertaken, showing good agreement with the stability studies. Fig. 8 shows the 3d transitions added to Fig. 5 to provide a more complete transition map.
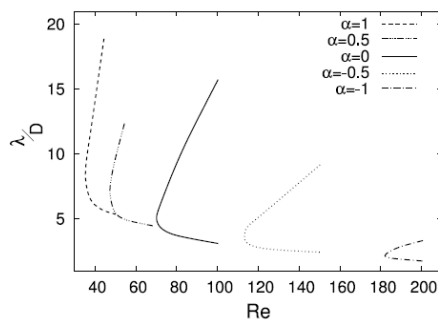

Figure 7: Rolling cylinder: curves of neutral stability (spanwise wavelength, λ, versus Reynolds number, Re, for different rotation rates, α) for which the growth rate is zero, indicating the transition to three-dimensional flow.
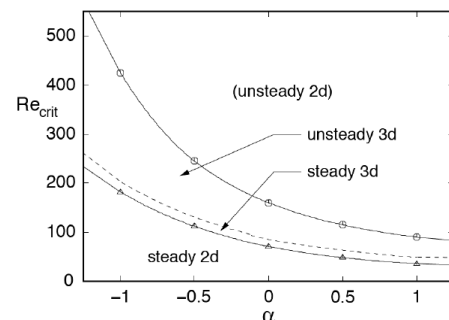

Figure 8: Transition map showing the critical Reynolds number, Re_c, for transition from 2d steady to 2d unsteady, from 2d steady to 3d steady, and from 3d steady to 3d unsteady.

Tandem cylinders

The wake structures, transitions and lift and drag forces on cylinders translating and spinning in tandem are being predicted using the spectral element method for a range of Reynolds numbers, Re, rotation rates, α, and separation, *S*. Examples for 3 rotation rates, α = 1, 0, and -1, Re = 200 and *S/D* = 5 are shown in Fig. 8.

The critical separation distances have been determined for which the nature of the flow changes. For example, as the separation, *S*, is increased, the wake from the first cylinder undergoes transition from steady flow to unsteady flow, increasing the fluctuating forces on the downstream cylinder. The lift and drag forces on the downstream cylinder are greatly influenced by the wake from the upstream cylinder, even at surprisingly large separation distances. Clockwise rotation of the cylinders has a stabilising effect on the flow, i.e., reducing unsteadiness, and anti-clockwise rotation has a destabilising effect.

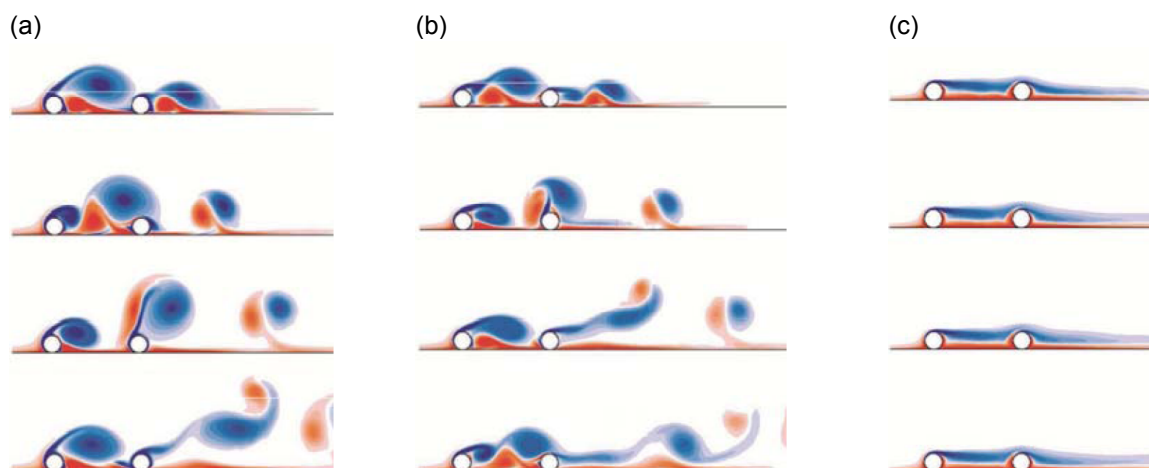More results of the tandem cylinders will be shown at the conference.

(a)   (b)   (c)

Figure 8: Vorticity plots of wakes of tandem cylinders, both translating on wall at Re = 200 and *S/D* = 5, with rotation rates (a) α = 1, (b) α = 0, and (c) α = -1.

REFERENCES

1. Bearman, P.W. & Zdravkovich, M.M. 1978 Flow around a circular cylinder near a plane boundary. Journal of Fluid Mechanics 89, 33–47.
2. Bhattacharyya, S., Mahapatra, S. & Smith, F.T. 2004 Fluid flow due to a cylinder rolling along ground. Journal of Fluids and Structures 19, 511–523.,
3. Cheng, M. & Luo, L.-S. 2007 Characteristics of two-dimensional flow around a rotating circular cylinder near a plane wall. Physics of Fluids 19, 063601–1–063601–17.
4. Karniadakis, G.E., Israeli, M. & Orszag, S.A. 1991 High-order splitting methods for the incompressible Navier-Stokes equations. *Journal of Computational Physics* 97, 414-443.
5. Magarvey, R.H. & Bishop, R.L. 1961 Transition ranges for three-dimensional wakes. Canadian Journal of Physics 39, 1418–1422.
6. Mittal, S. 2004 Three-dimensional instabilities in flow past a rotating cylinder. Journal of Applied Mechanics 71, 89–95.
7. Ormières, D. & Provansal, M. 1999 Transition to turbulence in the wake of a sphere. Physical Review Letters 83 (1), 80–83.
8. Pruppacher, H.R., Le Clair, B.P. & Hamielec, A.E. 1970 Some relations between drag and flow pattern of viscous flow past a sphere and a cylinder at low and intermediate Reynolds numbers. Journal of Fluid Mechanics 4, 781–790.
9. Roshko, A. 1954 On the development of turbulent wakes from vortex streets. Tech. Rep. 1191. National Advisory Committee for Aeronautics.
10. Stewart, B.E., Leweke, T., Hourigan, K. & Thompson, M.C. 2008 Wake formation behind a rolling sphere. Physics of Fluids 20, 071704.
11. Stewart, B.E., Thompson, M.C., Leweke, T. & Hourigan, K. 2010a Numerical and experimental studies of the rolling sphere wake. Journal of Fluid Mechanics, 643, 137–162.
12. Stewart, B.E., Thompson, M.C., Leweke, T. & Hourigan, K. 2010b The wake behind a cylinder rolling on a wall at varying rotation rates. Journal of Fluid Mechanics (in press).
13. Thompson, M., Hourigan, K. & Sheridan, J. 1996 Three-dimensional instabilities in the wake of a circular cylinder. Experimental Thermal and Fluid Science 12, 190–196.